IN-34
111055

NASA Contractor Report 189669
ICASE Report No. 92–28

P.17

ICASE

PREDICTING EQUILIBRIUM STATES WITH REYNOLDS STRESS CLOSURES IN CHANNEL FLOW AND HOMOGENEOUS SHEAR FLOW

R. Abid
C. G. Speziale

Contract Nos. NAS1–18605 and NAS1–19480
June 1992

Institute for Computer Applications in Science and Engineering
NASA Langley Research Center
Hampton, Virginia 23665–5225

Operated by the Universities Space Research Association

National Aeronautics and
Space Administration

Langley Research Center
Hampton, Virginia 23665-5225

PREDICTING EQUILIBRIUM STATES WITH REYNOLDS STRESS CLOSURES IN CHANNEL FLOW AND HOMOGENEOUS SHEAR FLOW

R. Abid
High Technology Corporation
NASA Langley Research Center
Hampton, VA 23665

C. G. Speziale*
Institute for Computer Applications in Science and Engineering
NASA Langley Research Center
Hampton, VA 23665

ABSTRACT

Turbulent channel flow and homogeneous shear flow have served as basic building block flows for the testing and calibration of Reynolds stress models. In this paper, a direct theoretical connection is made between homogeneous shear flow in equilibrium and the log-layer of fully-developed turbulent channel flow. It is shown that if a second-order closure model is calibrated to yield good equilibrium values for homogeneous shear flow it will also yield good results for the log-layer of channel flow provided that the Rotta coefficient is not too far removed from one. Most of the commonly used second-order closure models introduce an ad hoc wall reflection term in order to mask deficient predictions for the log-layer of channel flow that arise either from an inaccurate calibration of homogeneous shear flow or from the use of a Rotta coefficient that is too large. Illustrative model calculations are presented to demonstrate this point which has important implications for turbulence modeling.

*Research was supported by the National Aeronautics and Space Administration under NASA Contract Nos. NAS1-18605 and NAS1-19480 while the second author was in residence at the Institute for Computer Applications in Science and Engineering (ICASE), NASA Langley Research Center, Hampton, VA 23665.

1. INTRODUCTION

Turbulence models have been calibrated and tested using a variety of benchmark turbulent flows among which homogeneous shear flow and channel flow have played a central role. Typically these two flows are treated as separate tests that are completely independent. Starting with the work of Launder, Reece and Rodi[1], the pressure-strain correlation of turbulence – which forms a pivotal part of second-order closure models – has been calibrated based on the equilibrium Reynolds stress anisotropies in homogeneous shear flow. An ad hoc wall reflection term is then added to the pressure-strain model to yield good predictions for the log-layer of fully-developed turbulent channel flow. There are several disturbing features about the resulting model: the wall reflection term plays an important role far into the interior of the channel and it depends in an empirical manner on the normal distance from the wall. The latter deficiency makes it virtually impossible to systematically apply second-order closure models to turbulent wall-bounded flows in complex geometries containing sharp corners. This, as well as other near-wall problems, has impeded progress in the application of second-order closures to the turbulent flows of technological interest.

In this paper, it is shown that a second-order closure model will yield the *same* equilibrium Reynolds stress anisotropies in homogeneous shear flow and in the log-layer of channel flow if the slow pressure-strain correlation is represented by a Rotta[2] type of return-to-isotropy model with a coefficient of one. Since experiments[3,4] indicate that the Reynolds stress anisotropies for these two problems are close to one another, it follows that if a second-order closure model yields good equilibrium values for homogeneous shear flow it will also yield good results for the log-layer of channel flow provided that the Rotta coefficient is not too far removed from one. Illustrative calculations will be presented for four independent pressure-strain models – which include the models of Launder, Reece and Rodi[1], Shih and Lumley[5], Fu, Launder and Tselepidakis[6], and Speziale, Sarkar and Gatski[7] – in order to demonstrate this point. Some rather surprising results are obtained concerning the performance of these models in channel flow. In addition, a crucial compatibility condition for the turbulent diffusion coefficient in the transport equation for the dissipation rate is elaborated on. The important implications that these results have for the development of improved second-order closure models are discussed in detail.

2. THEORETICAL ANALYSIS

We consider incompressible turbulent flows for which the Reynolds-averaged Navier-

Stokes equations take the form

$$\frac{\partial \overline{u}_i}{\partial t} + \overline{u}_j \frac{\partial \overline{u}_i}{\partial x_j} = -\frac{\partial \overline{p}}{\partial x_i} + \nu \nabla^2 \overline{u}_i - \frac{\partial \tau_{ij}}{\partial x_j} \tag{1}$$

$$\boldsymbol{\nabla} \cdot \overline{\boldsymbol{u}} = 0 \tag{2}$$

where $\overline{u}_i$ is the mean velocity, $\overline{p}$ is the mean kinematic pressure, $\tau_{ij} \equiv \overline{u_i' u_j'}$ is the Reynolds stress tensor, and ν is the kinematic viscosity of the fluid. Here, the Einstein summation convention applies to repeated indices, an overbar represents an ensemble mean, and a prime represents a fluctuating quantity. The Reynolds stress tensor is a solution of the transport equation[8]

$$\frac{D\tau_{ij}}{Dt} = -\tau_{ik}\frac{\partial \overline{u}_j}{\partial x_k} - \tau_{jk}\frac{\partial \overline{u}_i}{\partial x_k} + \Pi_{ij} - \frac{2}{3}\varepsilon\delta_{ij} - \mathcal{D}_{ij}^T \tag{3}$$

at high Reynolds numbers where

$$\Pi_{ij} = \overline{p'\left(\frac{\partial u_i'}{\partial x_j} + \frac{\partial u_j'}{\partial x_i}\right)}, \quad \varepsilon = \nu \overline{\frac{\partial u_i'}{\partial x_j}\frac{\partial u_i'}{\partial x_j}}$$

$$\mathcal{D}_{ij}^T = \frac{\partial}{\partial x_k}(\overline{u_i' u_j' u_k'} + \overline{p' u_i'}\delta_{jk} + \overline{p' u_j'}\delta_{ik})$$

are, respectively, the pressure-strain correlation, turbulent dissipation rate, and turbulent diffusion term; $D/Dt \equiv \partial/\partial t + \overline{\boldsymbol{u}} \cdot \boldsymbol{\nabla}$ denotes the mean convective time rate and Kolmogorov's assumption of local isotropy has been invoked.

The two equilibrium turbulent shear flows to be considered are unidirectional with the mean velocity gradient tensor

$$\frac{\partial \overline{u}_i}{\partial x_j} = S\delta_{i1}\delta_{j2} \tag{4}$$

where $S \equiv d\overline{u}/dy$ (see Figure 1). For homogeneous shear flow, S is a constant, whereas for the log-layer of turbulent channel flow, $S = u_\tau/\kappa y$ where u_τ is the friction velocity and κ is the von Kármán constant (in more familiar terms, $u^+ = (1/\kappa)\ell n\ y^+ + 5$ in the log-layer where $u^+ = \overline{u}/u_\tau$ and $y^+ = y u_\tau/\nu$). In channel flow, the mean convective terms are identically zero and within the log-layer, turbulence production equals dissipation ($\mathcal{P} = \varepsilon$) and, hence, the molecular and turbulent diffusion terms in (3) can be neglected[9]. Consequently, the anisotropy tensor $b_{ij} \equiv (\tau_{ij} - \frac{2}{3}K\delta_{ij})/2K$ and shear parameter SK/ε (where $K = \frac{1}{2}\tau_{ii}$ is the turbulent kinetic energy) achieve constant equilibrium values in the log-layer that are independent of the boundary conditions. In homogeneous shear flow the molecular and turbulent diffusion terms in (3) are identically zero and each component of the Reynolds stress tensor grows exponentially at the same rate so that the anisotropy tensor b_{ij} and shear parameter SK/ε achieve equilibrium values that are independent of the initial conditions[10].

It is thus clear that the structural equilibrium in homogeneous shear flow and the production-equals-dissipation equilibrium in the log-layer of turbulent channel flow are each characterized by the constraints SK/ε = constant and b_{ij} = constant. The latter constraint is equivalent to $Db_{ij}/Dt = 0$, or

$$\frac{D\tau_{ij}}{Dt} = (\mathcal{P} - \varepsilon)\frac{\tau_{ij}}{K} \tag{5}$$

where $\mathcal{P} \equiv -\tau_{12}S$ is the turbulence production. The substitution of (4) and (5) into (3), with vanishing turbulent diffusion terms, yields the equation

$$\frac{\tau_{ij}}{K}\left(\frac{\mathcal{P}}{\varepsilon} - 1\right)\frac{\varepsilon}{SK} = -\frac{\tau_{i2}}{K}\delta_{j1} - \frac{\tau_{j2}}{K}\delta_{i1} + \frac{\Pi_{ij}}{SK} - \frac{2}{3}\frac{\varepsilon}{SK}\delta_{ij} \tag{6}$$

which is valid for an equilibrium homogeneous shear flow and for the log-layer of channel flow. We will consider second-order closure models where

$$\Pi_{ij} = \Pi_{ij}^{(S)} + \Pi_{ij}^{(R)} \tag{7}$$

and the slow pressure-strain correlation $\Pi_{ij}^{(S)}$ is represented by a Rotta[2] type of return-to-isotropy model

$$\Pi_{ij}^{(S)} = -C_1\frac{\varepsilon}{K}\left(\tau_{ij} - \frac{2}{3}K\delta_{ij}\right) \tag{8}$$

whereas the rapid pressure-strain correlation $\Pi_{ij}^{(R)}$ is modeled in the general form

$$\Pi_{ij}^{(R)} = K\mathcal{M}_{ijkl}(\boldsymbol{b})\frac{\partial \overline{u}_k}{\partial x_l}. \tag{9}$$

Here, both the Rotta coefficient C_1 and the fourth-rank tensor $\mathcal{M}_{ijkl}$ can be functions of b_{ij} (see the Appendix).

If we make use of the fact that

$$\frac{\mathcal{P}}{\varepsilon} = -\frac{\tau_{12}}{K}\frac{SK}{\varepsilon}, \tag{10}$$

along with (8)-(9), it is straightforward to show that (6) can be written in the equivalent form

$$\frac{\tau_{ij}}{K}\frac{\tau_{12}}{K} - \frac{\tau_{i2}}{K}\delta_{j1} - \frac{\tau_{j2}}{K}\delta_{i1} + \Pi_{ij}^{*(R)} + (C_1 - 1)\left(\frac{\tau_{ij}}{K} - \frac{2}{3}\delta_{ij}\right)\left(\frac{\tau_{12}}{K}\right)\left(\frac{\mathcal{P}}{\varepsilon}\right)^{-1} = 0 \tag{11}$$

where $\Pi_{ij}^{*(R)} \equiv \mathcal{M}_{ij12}(\boldsymbol{b})$ is specified by the pressure-strain model chosen. Hence, since τ_{ij}/K is directly related to b_{ij}, it then becomes clear that a closed set of nonlinear algebraic equations for the non-zero components of the anisotropy tensor (b_{11}, b_{12}, b_{22} and b_{33}) are obtained once $\mathcal{P}/\varepsilon$ is specified. Since $\mathcal{P}/\varepsilon = 1$ for the log-layer of channel flow and $\mathcal{P}/\varepsilon \approx 1.8$ for an equilibrium homogeneous shear flow, it is clear that the same equilibrium values will

be obtained for these respective problems only when the Rotta coefficient $C_1 = 1$ (the limit in which the dependence of b_{ij} on $\mathcal{P}/\varepsilon$ is eliminated in (11)). It is also clear that this result carries over to the more general tensorially quadratic return models of the form[7]

$$\Pi_{ij}^{(S)} = -2C_1\varepsilon b_{ij} + 6(C_1 - 1)\varepsilon\left(b_{ik}b_{kj} - \frac{1}{3}b_{kl}b_{kl}\delta_{ij}\right) \tag{12}$$

where the coefficient C_1 can be a function of the second and third invariants of b_{ij}. This leads us to the central result of this paper: *A second-order closure model will yield approximately the same equilibrium values for b_{ij} in homogeneous shear flow and in the log-layer of channel flow provided that Rotta coefficient is sufficiently close to one.* In the next section, model calculations will be presented to illustrate that with a Rotta constant C_1 as large as 1.7 it is possible to obtain good results for both channel flow and homogeneous shear flow without an ad hoc wall reflection term.

3. ILLUSTRATIVE MODEL CALCULATIONS

Calculations will now be presented for four pressure-strain models: the Launder, Reece and Rodi (LRR) model[1], the Shih-Lumley (SL) model[5], the Fu, Launder and Tselepidakis (FLT) model[6], and the Speziale, Sarkar and Gatski (SSG) model[7] (see the Appendix for more details on the models). The equilibrium values corresponding to these models are obtained by substituting a given pressure-strain model into (6) and solving the resulting nonlinear algebraic equations numerically after (10) is made use of to eliminate SK/ε. For channel flow, $\mathcal{P}/\varepsilon$ is set equal to 1 whereas for homogeneous shear flow, $\mathcal{P}/\varepsilon$ is taken to be 1.8. In Table 1, the equilibrium Reynolds stress anisotropies b_{ij} and shear parameter SK/ε obtained from the various models are compared with the experimental data of Tavoularis and Karnik[3] for homogeneous shear flow. Several observations concerning these results are noteworthy: (a) the SSG and FLT models are, by far, in the best agreement with the experimental data for homogeneous shear flow, (b) the LRR model does not do as well since it was calibrated based on the older and less complete experimental data of Champagne, Harris and Corrsin[11], and (c) the SL model performs the worst since, in its calibration, homogeneous shear flow was not directly accounted for. In Table 2, the corresponding model predictions for the log-layer of channel flow are compared with experimental data[4] (here, an average is taken of the log-layer values which vary somewhat with y^+). Apparently, only the SSG model yields equilibrium values that are in close range of the experimental data. The FLT model – which performs well in homogeneous shear flow – does not do quite as well in channel flow. This is a direct consequence of the theoretical result derived in the previous section. If a model yields accurate results in homogeneous shear flow, good results will automatically follow for the log-layer of channel flow provided that the Rotta coefficient is sufficiently close to one.

In the SSG model, the Rotta coefficient $C_1 = 1.7$ is sufficiently close to one to guarantee that

$$\frac{(C_1 - 1)\|b_{ij}\| \cdot \|b_{12}\|}{\|\Pi_{ij}^{*(R)}\|\mathcal{P}/\varepsilon} \ll 1 \tag{13}$$

for all i and j where $\|\cdot\|$ is any suitable norm (this is a sufficient condition, that follows directly from (11), which guarantees that results for b_{ij} in homogeneous shear flow and channel flow will be close to one another as indicated by experiments). On the other hand, due to its nonlinear dependence on the invariants of b_{ij}, the Rotta coefficient $C_1 \approx 3$ for the FLT model which explains why the normal Reynolds stress anisotropies in channel flow differ by as much as 25% from their counterparts for homogeneous shear flow. The same is true for the SL model since its Rotta coefficient C_1 is approximately 5 in homogeneous shear flow (however, unlike the FLT model, the SL model renders inaccurate predictions for both homogeneous shear flow and channel flow). The LRR model has a sufficiently small Rotta coefficient $C_1 \approx 1.5$ so that the deviations between its predictions for b_{ij} in homogeneous shear flow and in channel flow are not fatal. The problem with this model is that it was not optimally calibrated for homogeneous shear flow – a deficiency that is tied to the fact that this model was developed before the more accurate experimental data became available which clearly indicated that production exceeds dissipation. In the calibration of the LRR model, the production was set equal to the dissipation for homogeneous shear flow[1].

Some comments are in order concerning how these results compare with the more detailed model calculations of homogeneous shear flow by Speziale and co-workers[7,10,12] and the recent systematic calculations of channel flow by Demuren and Sarkar[13]. For these more complete calculations, the Reynolds stress transport equation (3) must be supplemented with a modeled transport equation for the turbulent dissipation rate ε which is typically taken to be of the form[1]

$$\frac{D\varepsilon}{Dt} = C_{\varepsilon 1}\frac{\varepsilon}{K}\mathcal{P} - C_{\varepsilon 2}\frac{\varepsilon^2}{K} + \frac{\partial}{\partial x_i}\left(C_\varepsilon \tau_{ij}\frac{K}{\varepsilon}\frac{\partial \varepsilon}{\partial x_j}\right) \tag{14}$$

where $C_{\varepsilon 1}, C_{\varepsilon 2}$ and C_ε are constants whose values vary from one model to the next. For homogeneous shear flow, the diffusion terms in (14) vanish. Since, $DK/Dt = \mathcal{P} - \varepsilon$ for any homogeneous turbulence, it then follows that an equilibrium state is achieved where

$$\frac{\mathcal{P}}{\varepsilon} = \frac{C_{\varepsilon 2} - 1}{C_{\varepsilon 1} - 1} \tag{15}$$

in the limit as $t \to \infty$ (see Speziale and Mac Giolla Mhuiris[10]). Hence, the equilibrium values for the various models given on Table 1 are identical to those that would be obtained from full Reynolds stress transport calculations using the model (14) with $(C_{\varepsilon 2} - 1)/(C_{\varepsilon 1} - 1) = 1.8$. Since most of the models do not employ precisely the same values for $C_{\varepsilon 1}$ and $C_{\varepsilon 2}$, there

are some small differences between the equilibrium values displayed in Table 1 and those published previously[7,10,12]. However, the calculations presented herein for homogeneous shear flow actually form a more objective basis for the comparison of Reynolds stress models since $\mathcal{P}/\varepsilon$ is set to a common experimental equilibrium value and the calculations are then freed from dependence on the model chosen for the turbulent dissipation rate.

There is also a compatibility relation for the log-layer of channel flow that needs to be discussed. Since in the log-layer $du^+/dy^+ = \varepsilon^+ = 1/\kappa y^+$ and b_{ij} as well as K are constant, it follows that

$$C_\varepsilon = \frac{8(C_{\varepsilon 1} - C_{\varepsilon 2})b_{12}^3}{\kappa^2(2b_{22} + \frac{2}{3})} \tag{16}$$

for the modeled dissipation rate equation to be consistent. Full Reynolds stress calculations of channel flow with models that satisfy the consistency constraint (16) will be in close approximate agreement with our calculations. The minor differences between the equilibrium values given in Table 2 based on our log-layer analysis and those obtained by Demuren and Sarkar[13] based on full Reynolds stress calculations are due to turbulent diffusion effects and the fact that some of the models considered herein violate constraint (16). Since $C_{\varepsilon 2} - C_{\varepsilon 1}$ is in the range of 0.40 - 0.45 for most of the commonly used models, it follows that in order to yield a von Kármán constant of $\kappa = 0.41$ (with the approximate log-layer values of $b_{12} \approx -0.15$ and $b_{22} \approx -0.14$), the value of C_ε chosen should be in the range of 0.16 - 0.18. This constraint should be made use of more carefully in the future formulation of second-order closure models.

Finally, some comments are in order concerning the wall reflection term that is added to many pressure-strain models in second-order closures to yield acceptable predictions for the log-layer of turbulent channel flow. Typically, the wall reflection correction Π_{ij}^w is of the general form[1]

$$\Pi_{ij}^w = \left[C_{w1}\frac{\varepsilon}{K}\left(\tau_{ij} - \frac{2}{3}K\delta_{ij}\right) + C_{w2}\overline{\Pi}_{ij}^{(R)}\right]\frac{K^{3/2}}{\varepsilon y} \tag{17}$$

where $\overline{\Pi}_{ij}^{(R)}$ is directly related to the rapid pressure-strain model in the absence of walls, y is the distance normal to the wall, and C_{w1} and C_{w2} are empirical constants. Since

$$\frac{K^{3/2}}{\varepsilon y} = \kappa K^{+3/2} \approx 2.5 \tag{18}$$

in the log-layer, and since C_{w1} is typically chosen to be in the range of 0.1 - 1.0, it follows that the wall reflection term makes a *significant* contribution to the slow pressure-strain correlation (this needs to be the case for many pressure-strain models due to their poor performance in channel flow as shown in Table 2). The problem with this is clear. At high Reynolds numbers the log-layer extends far into the interior of the channel. To have an

ad hoc correction – that depends on the normal distance from the wall – play a significant role far into the interior of the fluid is dangerous. It seriously diminishes the possibility of applying these models in complex geometries with corners where the normal distance y from the wall is not uniquely defined.

4. CONCLUSIONS

A direct theoretical connection between the log-layer of turbulent channel flow and homogeneous shear flow in equilibrium has been established. These flows have traditionally been treated as being independent tests since in the former flow there is a production-equals-dissipation equilibrium, with bounded turbulent kinetic energy and dissipation, whereas in the latter flow, production exceeds dissipation so that the turbulent kinetic energy and dissipation rate grow exponentially with time. However, both flows have a common theoretical thread that connects them: the anisotropy tensor b_{ij} and shear parameter SK/ε achieve equilibrium values that are independent of the initial/boundary conditions. It was shown that in the limit as the Rotta coefficient goes to one, a second-order closure model will yield the *same* equilibrium values for b_{ij} in the log-layer of channel flow and in homogeneous shear flow. Furthermore, it was demonstrated that with a Rotta coefficient C_1 as large as 1.7 – which is a value that allows for the collapse of a significant range of return to isotropy data[7] – a model that was calibrated to yield good equilibrium values for homogeneous shear flow (the SSG model) also performs well in the log-layer of channel flow without ad hoc corrections. Hence, it appears that a model can be calibrated to perform well in both flows provided that the Rotta coefficient is not too far removed from one.

The results obtained in this study have important implications for turbulence modeling. It is rather disquieting how poorly many of the currently popular second-order closure models perform in the log-layer of turbulent channel flow. These deficiencies have their origin in two major sources: an inaccurate calibration of the model for homogeneous shear flow or the use of a Rotta coefficient that is too far removed from one (a state of affairs that has arisen from the introduction of an empirical nonlinear dependence of C_1 on the invariants of b_{ij}). The introduction of an ad hoc wall reflection term to alleviate this problem has seriously inhibited the ability to apply second-order closure models to turbulent flows in complex geometries. Since turbulent channel flow is dynamically similar to a two-dimensional equilibrium turbulent boundary layer – which forms a cornerstone for many practical engineering applications – it is crucial to get this flow right without ad hoc corrections that make the model geometry-dependent. The results of this study clearly show that it is possible to do this. More attention needs to be paid to this issue in the future if second-order closure models are to have an impact on the calculation of complex wall-bounded turbulent flows.

ACKNOWLEDGEMENT

The first author (RA) would like to acknowledge the support of NASA Langley Research Center.

REFERENCES

[1]B. E. Launder, G. Reece and W. Rodi, "Progress in the development of a Reynolds-stress turbulence closure," *J. Fluid Mech.* **68**, 537 (1975).

[2]J. C. Rotta, "Statistische theorie nichthomogener turbulenz," *Z. Phys.* **129**, 547 (1951).

[3]S. Tavoularis and U. Karnik, "Further experiments on the evolution of turbulent stresses and scales in uniformly sheared turbulence," *J. Fluid Mech.* **204**, 457 (1989).

[4]J. Laufer, "Investigation of turbulent flow in a two-dimensional channel," *NACA TN 1053* (1951).

[5]T. H. Shih and J. L. Lumley, "Modeling of pressure correlation terms in Reynolds stress and scalar flux equations," *Cornell University Technical Report FDA-85-3* (1985).

[6]S. Fu, B. E. Launder and D. P. Tselepidakis, "Accommodating the effects of high strain rates in modelling the pressure-strain correlation," *UMIST Mechanical Engineering Department Report TFD/87/5* (1987).

[7]C. G. Speziale, S. Sarkar and T. B. Gatski, "Modeling the pressure-strain correlation of turbulence: An invariant dynamical systems approach," *J. Fluid Mech.* **227**, 245 (1991).

[8]W. C. Reynolds, "Fundamentals of turbulence for turbulence modeling and simulation," *Lecture Notes for Von Kármán Institute, AGARD Report No. 755* (NATO, Specialized Printing Services, Loughton, Essex, 1987).

[9]P. Bradshaw, T. Cebeci and J. H. Whitelaw, *Engineering Calculation Methods for Turbulent Flow*, (Academic, New York, 1981).

[10]C. G. Speziale and N. Mac Giolla Mhuiris, "On the prediction of equilibrium states in homogeneous turbulence," *J. Fluid Mech.* **209**, 591 (1989).

[11]F. H. Champagne, V. G. Harris and S. Corrsin, "Experiments on nearly homogeneous turbulent shear flow," *J. Fluid Mech.* **41**, 81 (1970).

[12]C. G. Speziale, T. B. Gatski and N. Mac Giolla Mhuiris, "A critical comparison of turbulence models for homogeneous turbulent shear flows in a rotating frame," *Phys. Fluids A* **2**, 1678 (1990).

[13]A. O. Demuren and S. Sarkar, "Systematic study of Reynolds stress closure models in the computations of plane channel flows," *ICASE Report 92-19*, NASA Langley Research Center (1992).

APPENDIX

The detailed form of the pressure-strain models considered in this paper are as follows:

Launder, Reece & Rodi Model

$$\begin{aligned}\Pi_{ij} &= -2C_1\varepsilon b_{ij} + \frac{4}{5}K\overline{S}_{ij} + C_2K\left(b_{ik}\overline{S}_{jk} + b_{jk}\overline{S}_{ik}\right. \\ &\left. -\frac{2}{3}b_{kl}\overline{S}_{kl}\delta_{ij}\right) + C_3K(b_{ik}\overline{W}_{jk} + b_{jk}\overline{W}_{ik})\end{aligned} \tag{A1}$$

where

$$\overline{S}_{ij} = \frac{1}{2}\left(\frac{\partial\overline{u}_i}{\partial x_j} + \frac{\partial\overline{u}_j}{\partial x_i}\right), \quad \overline{W}_{ij} = \frac{1}{2}\left(\frac{\partial\overline{u}_i}{\partial x_j} - \frac{\partial\overline{u}_j}{\partial x_i}\right) \tag{A2}$$

$$C_1 = 1.5,\ C_2 = 1.75,\ C_3 = 1.31 \tag{A3}$$

Shih & Lumley Model

$$\begin{aligned}\Pi_{ij} &= -\beta\varepsilon b_{ij} + \frac{4}{5}K\overline{S}_{ij} + 12\alpha_5K\left(b_{ik}\overline{S}_{jk} + b_{jk}\overline{S}_{ik}\right. \\ &\left. -\frac{2}{3}b_{kl}\overline{S}_{kl}\delta_{ij}\right) + \frac{4}{3}(2 - 7\alpha_5)K(b_{ik}\overline{W}_{jk} + b_{jk}\overline{W}_{ik}) \\ &+\frac{4}{5}K(b_{il}b_{lm}\overline{S}_{jm} + b_{jl}b_{lm}\overline{S}_{im} - 2b_{ik}\overline{S}_{kl}b_{lj} \\ &-3b_{kl}\overline{S}_{kl}b_{ij}) + \frac{4}{5}K(b_{il}b_{lm}\overline{W}_{jm} + b_{jl}b_{lm}\overline{W}_{im})\end{aligned} \tag{A4}$$

where

$$\beta = 2 + \frac{F}{9}\exp(-7.77/\sqrt{Re_t})\{72/\sqrt{Re_t} + 80.1\ ln[1 + 62.4(-II + 2.3III)]\} \tag{A5}$$

$$F = 1 + 9II + 27III \tag{A6}$$

$$II = -\frac{1}{2}b_{ij}b_{ij}, \quad III = \frac{1}{3}b_{ij}b_{jk}b_{ki} \tag{A7}$$

$$Re_t = \frac{4}{9}\frac{K^2}{\nu\varepsilon} \tag{A8}$$

$$\alpha_5 = \frac{1}{10}\left(1 + \frac{4}{5}F^{\frac{1}{2}}\right) \tag{A9}$$

Fu, Launder & Tselepidakis Model

$$\begin{aligned}\Pi_{ij} &= \beta_1\varepsilon b_{ij} + \beta_2\varepsilon\left(b_{ik}b_{kj} - \frac{1}{3}b_{kl}b_{kl}\delta_{ij}\right)\\ &+\frac{4}{5}K\overline{S}_{ij} + 1.2K\left(b_{ik}\overline{S}_{jk} + b_{jk}\overline{S}_{ik} - \frac{2}{3}b_{kl}\overline{S}_{kl}\delta_{ij}\right)\\ &+\frac{26}{15}K(b_{ik}\overline{W}_{jk} + b_{jk}\overline{W}_{ik}) + \frac{4}{5}K(b_{ik}b_{kl}\overline{S}_{jl}\\ &+b_{jk}b_{kl}\overline{S}_{il} - 2b_{ik}\overline{S}_{kl}b_{lj} - 3b_{kl}\overline{S}_{kl}b_{ij})\\ &+\frac{4}{5}K\left(b_{ik}b_{kl}\overline{W}_{jl} + b_{jk}b_{kl}\overline{W}_{il}\right) - \frac{14}{5}K\left[8II(b_{ik}\overline{W}_{jk}\right.\\ &\left.+b_{jk}\overline{W}_{ik}\right) + 12\left(b_{ik}b_{kl}\overline{W}_{lm}b_{mj} + b_{jk}b_{kl}\overline{W}_{lm}b_{mi}\right)\Big]\end{aligned} \tag{A10}$$

where

$$\beta_1 = 120IIF^{1/2} + 2F^{1/2} - 2,\ \beta_2 = 144IIF^{1/2} \tag{A11}$$

Speziale, Sarkar & Gatski Model

$$\begin{aligned}\Pi_{ij} &= -(2C_1\varepsilon + C_1^*\mathcal{P})b_{ij} + C_2\varepsilon\left(b_{ik}b_{kj} - \frac{1}{3}b_{kl}b_{kl}\delta_{ij}\right) + (C_3 - C_3^*II_b^{\frac{1}{2}})K\overline{S}_{ij}\\ &+C_4K\left(b_{ik}\overline{S}_{jk} + b_{jk}\overline{S}_{ik} - \frac{2}{3}b_{kl}\overline{S}_{kl}\delta_{ij}\right) + C_5K(b_{ik}\overline{W}_{jk} + b_{jk}\overline{W}_{ik})\end{aligned} \tag{A12}$$

where

$$C_1 = 1.7,\ C_1^* = 1.80,\ C_2 = 4.2 \tag{A13}$$

$$C_3 = \frac{4}{5},\ C_3^* = 1.30,\ C_4 = 1.25 \tag{A14}$$

$$C_5 = 0.40,\ II_b = b_{ij}b_{ij} \tag{A15}$$

Equilibrium Values	LRR Model	SL Model	FLT Model	SSG Model	Experimental Data
b_{11}	0.152	0.120	0.196	0.218	0.21
b_{12}	-0.186	-0.121	-0.151	-0.164	-0.16
b_{22}	-0.119	-0.122	-0.136	-0.145	-0.14
b_{33}	-0.033	0.002	-0.060	-0.073	-0.07
SK/ε	4.83	7.44	5.95	5.50	5.0

Table 1. Comparison of the model predictions for the equilibrium values in homogeneous shear flow ($\mathcal{P}/\varepsilon = 1.8$) with the experimental data of Tavoularis and Karnik[3].

Equilibrium Values	LRR Model	SL Model	FLT Model	SSG Model	Experimental Data
b_{11}	0.129	0.079	0.141	0.201	0.22
b_{12}	-0.178	-0.116	-0.162	-0.160	-0.16
b_{22}	-0.101	-0.082	-0.099	-0.127	-0.15
b_{33}	-0.028	0.003	-0.042	-0.074	-0.07
SK/ε	2.80	4.30	3.09	3.12	3.1

Table 2. Comparison of the model predictions for the equilibrium values in the log-layer of turbulent channel flow ($\mathcal{P}/\varepsilon = 1$) with the mean experimental data of Laufer[4].

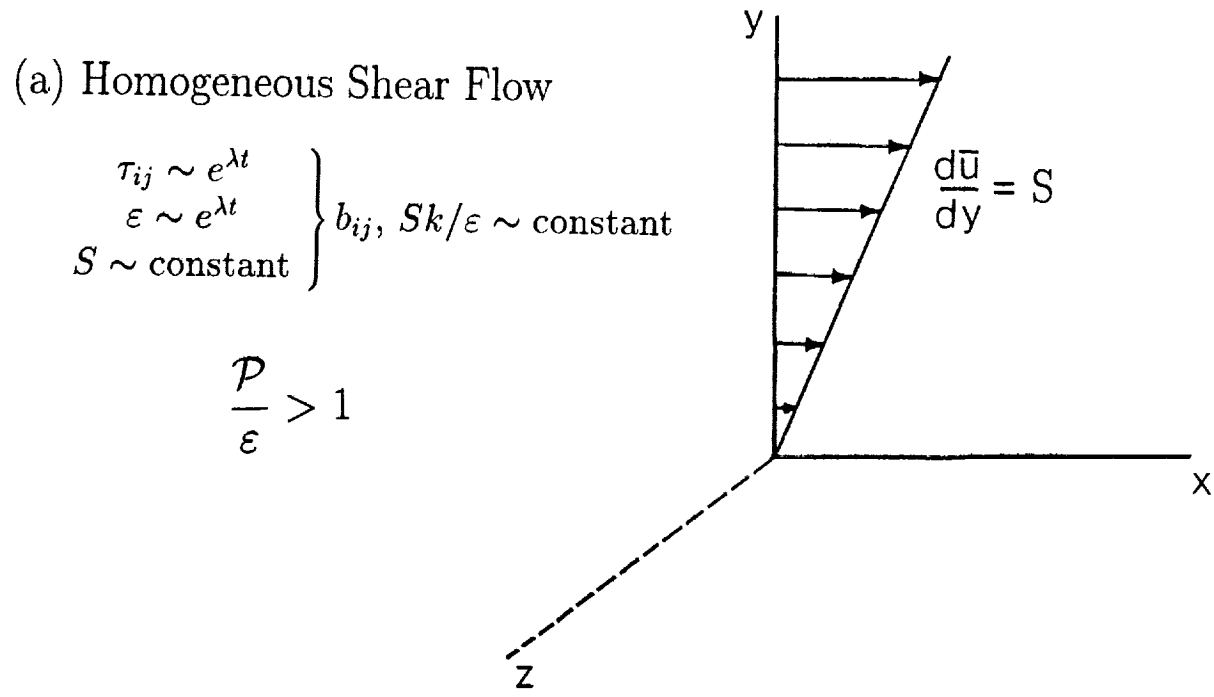

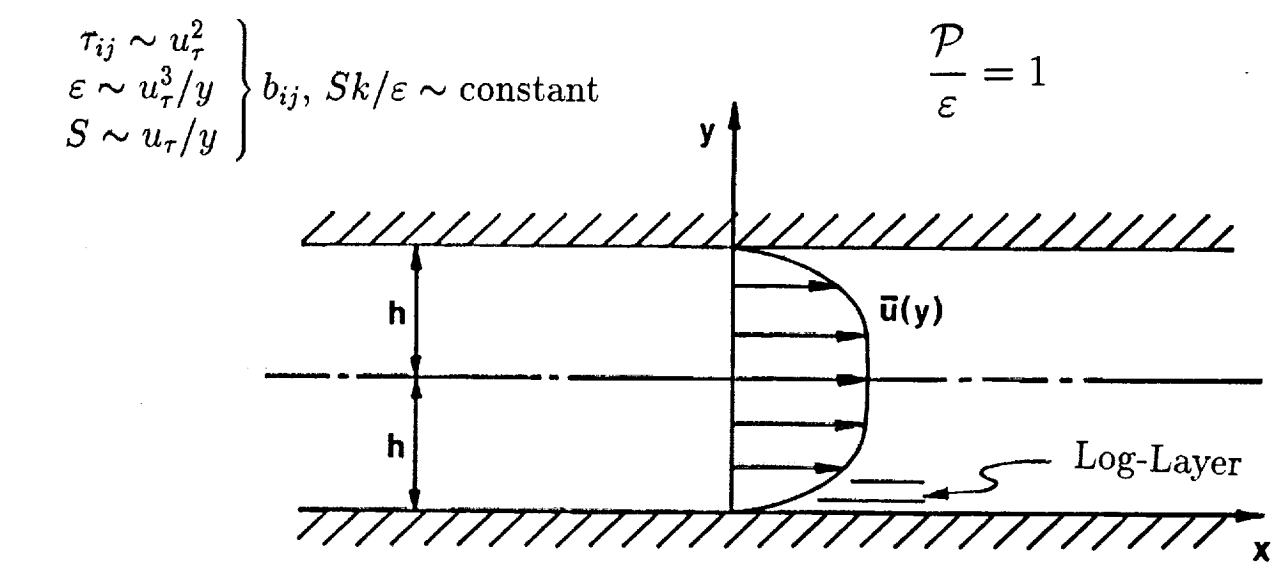

Figure 1. Schematic of the equilibrium turbulent flows: (a) Homogeneous shear flow and (b) log-layer of channel flow.

REPORT DOCUMENTATION PAGE

Form Approved
OMB No. 0704-0188

1. AGENCY USE ONLY *(Leave blank)*	2. REPORT DATE	3. REPORT TYPE AND DATES COVERED
	June 1992	Contractor Report

4. TITLE AND SUBTITLE
PREDICTING EQUILIBRIUM STATES WITH REYNOLDS STRESS CLOSURES IN CHANNEL FLOW AND HOMOGENEOUS SHEAR FLOW

5. FUNDING NUMBERS
C NAS1-18605
C NAS1-19480
WU 505-90-52-01

6. AUTHOR(S)
R. Abid
C. G. Speziale

7. PERFORMING ORGANIZATION NAME(S) AND ADDRESS(ES)
Institute for Computer Applications in Science and Engineering
Mail Stop 132C, NASA Langley Research Center
Hampton, VA 23665-5225

8. PERFORMING ORGANIZATION REPORT NUMBER
ICASE Report No. 92-28

9. SPONSORING/MONITORING AGENCY NAME(S) AND ADDRESS(ES)
National Aeronautics and Space Administration
Langley Research Center
Hampton, VA 23665-5225

10. SPONSORING/MONITORING AGENCY REPORT NUMBER
NASA CR-189669
ICASE Report No. 92-28

11. SUPPLEMENTARY NOTES
Langley Technical Monitor; Michael F. Card
Final Report
To be submitted to Physics of Fluids A

12a. DISTRIBUTION/AVAILABILITY STATEMENT
Unclassified - Unlimited

Subject Category 34

12b. DISTRIBUTION CODE

13. ABSTRACT *(Maximum 200 words)*

Turbulent channel flow and homogeneous shear flow have served as basic building block flows for the testing and calibration of Reynolds stress models. In this paper, a direct theoretical connection is made between homogeneous shear flow in equilibrium and the log-layer of fully-developed turbulent channel flow. It is shown that if a second-order closure model is calibrated to yield good equilibrium values for homogeneous shear flow it will also yield good results for the log-layer of channel flow provided that the Rotta coefficient is not too far removed from one. Most of the commonly used second-order closure models introduce an ad hoc wall reflection term in order to mask deficient predictions for the log-layer of channel flow that arise either from an inaccurate calibration of homogeneous shear flow or from the use of a Rotta coefficient that is too large. Illustrative model calculations are presented to demonstrate this point which has important implications for turbulence modeling.

14. SUBJECT TERMS
Turbulent channel flow; homogeneous shear flow; second-order closure models

15. NUMBER OF PAGES
16

16. PRICE CODE
A03

17. SECURITY CLASSIFICATION OF REPORT	18. SECURITY CLASSIFICATION OF THIS PAGE	19. SECURITY CLASSIFICATION OF ABSTRACT	20. LIMITATION OF ABSTRACT
Unclassified	Unclassified		